



Published in final edited form as:

Biochemistry. 2009 August 25; 48(33): 8051–8061. doi:10.1021/bi9007066.

## Stimulation of the maltose transporter ATPase by unliganded maltose binding protein

Alister D. Gould<sup>1</sup>, Patrick G. Telmer<sup>\*,1</sup>, and Brian H. Shilton<sup>†</sup>

Department of Biochemistry, The University of Western Ontario, 1151 Richmond St., London, Ontario Canada N6A 5C1

### Abstract

ATP hydrolysis by the maltose transporter (MalFGK<sub>2</sub>) is regulated by maltose binding protein (MBP). Binding of maltose to MBP brings about a conformational change from “open” to “closed” that leads to a strong stimulation of the MalFGK<sub>2</sub> ATPase. In this study we address the long-standing but enigmatic observation that unliganded MBP is also able to stimulate MalFGK<sub>2</sub>. Although the mechanism of this stimulation is not understood, it is sometimes attributed to a small amount of closed (but unliganded) MBP that may exist in solution. To gain insight into how MBP regulates the MalFGK<sub>2</sub> ATPase, we have investigated whether the open or the closed conformation of MBP is responsible for MalFGK<sub>2</sub> stimulation in the absence of maltose. The effect of MBP concentration on the stimulation of MalFGK<sub>2</sub> was assessed: for unliganded MBP, the apparent  $K_M$  for stimulation of MalFGK<sub>2</sub> was below 1  $\mu\text{M}$ , while for maltose-bound MBP, the  $K_M$  was approximately 15  $\mu\text{M}$ . We show that engineered MBP molecules in which the open-closed equilibrium has been shifted towards the closed conformation have a decreased ability to stimulate MalFGK<sub>2</sub>. These results indicate that stimulation of the MalFGK<sub>2</sub> ATPase by unliganded MBP does not proceed through a closed conformation and instead must operate through a different mechanism than stimulation by liganded MBP. One possible explanation is that the open conformation is able to activate the MalFGK<sub>2</sub> ATPase directly.

---

ATP Binding Cassette (ABC) transporters use the chemical energy of ATP hydrolysis to transport solutes across a membrane. ABC transporters can be divided into export systems and import systems, and a key question in both cases is the mechanism by which ATP binding and hydrolysis are regulated and coupled to substrate translocation. For ABC export systems, the substrate itself regulates the ATPase (1–3). ABC import systems, on the other hand, include a peripheral substrate binding protein, and the ATPase activity is regulated by interactions between the binding protein and the transmembrane components (4–6).

The *E. coli* maltose transporter is a tractable and well-studied ABC import system consisting of the membrane associated complex MalFGK<sub>2</sub> and peripheral extracellular maltose binding protein (MBP). MalF and MalG are integral membrane proteins; MalK<sub>2</sub> is a dimer of ABC subunits bound to MalFG on the cytoplasmic side of the membrane. Structures of isolated MalK<sub>2</sub> have been solved and from these it is known that ATP binds in the dimer interface and promotes a tight association of the subunits, bringing each ATP molecule in contact with catalytic residues from the opposite subunit (7). Once ATP hydrolysis takes place, the subunits dissociate, allowing release of ADP and inorganic phosphate (8). In the intact MalFGK<sub>2</sub>

---

†CORRESPONDING AUTHOR: bshilton@uwo.ca, Fax: 519-661-3175, Telephone: 519-661-4124.

\*current affiliation: Southern Crop Protection and Food Research Branch, Agriculture and Agrifood Canada, 1391 Sandford St., London, Ontario, Canada N5V 4T3

<sup>1</sup>These authors contributed equally to this work.

complex, these conformational changes are coupled to changes in MalFG (9–12) so that the maltose binding site in MalFG opens alternately to the periplasm or cytoplasm (12).

Stimulation of ATP hydrolysis by the binding protein must involve conformational changes that are transmitted from the extracellular surface through the transmembrane domains to the ATP binding cassettes on the cytoplasmic side. MBP and other Class I or II binding proteins consist of two domains connected by a flexible hinge, and ligand binding brings about a large structural change of the protein (13). This conformational change, from the “open” unliganded structure, to the “closed” liganded form, is critical for transport since only the ligand-bound conformation can fully stimulate the membrane ATPase (4,14). On this basis, the ligand-induced conformational change serves to ensure that futile cycles of ATP hydrolysis are avoided.

This picture is complicated by the enigmatic observation, in both the maltose and histidine transport systems, that ATP hydrolysis is stimulated, to a limited degree, by the *unliganded* binding protein (4,5). While there is no obvious physiological function for the ability of the unliganded binding protein to stimulate the membrane ATPase, it does raise questions about the mechanism of the stimulation. Specifically, it is not clear what conformation of MBP is responsible for the activation of the MalFGK<sub>2</sub> ATPase in the absence of maltose. On the one hand, unliganded MBP exists predominantly in an open conformation in solution (15,16), and therefore the open conformation represents a logical candidate for the activation. In support of this idea, during maltose transport and at the point where ATP is poised for hydrolysis, the open unliganded form is found tightly bound to MalFGK<sub>2</sub> (11,17). On the other hand, maltose transport requires an initial interaction with closed, maltose-bound MBP prior to opening and progression to the transition state for ATP hydrolysis. Therefore, the activation of the MalFGK<sub>2</sub> ATPase by unliganded MBP could be due to a small amount of a closed, unliganded form of MBP which exists in solution (18); the presence of such a solution conformation is supported by the crystallization of two other binding proteins in a closed, unliganded state (19,20). On this basis, a closed unliganded conformation might effect the same changes brought about by the closed *liganded* conformation. This model for stimulation of the ATPase by the binding protein could be termed “lock-and-key” since it is solely the conformation and the surface complementarity of the binding protein that is important for the interaction.

However, substrate binding affects not only the conformation, but also the stability and molecular dynamics of the binding protein. In the case of MBP, intrinsic tryptophan fluorescence and molecular dynamics simulations indicate that unliganded MBP has a somewhat dynamic structure, with the two domains moving relative to each other, in contrast to the ligand-bound form in which the relative positions of the domains appears to be fixed (21,22). Furthermore, the closed *unliganded* conformation has a much higher energy and lower stability than the closed, liganded form due to the absence of stabilizing non-covalent bonds between maltose and MBP (23). Thus, although a closed, unliganded conformation of MBP could, in principle, resemble the closed liganded form, it will be more dynamic and much less stable. On this basis, stimulation of the MalFGK<sub>2</sub> ATPase by a closed, unliganded conformation of MBP implies that the conformational stability of the binding protein is not critical for a productive interaction, and this has significant mechanistic implications for how conformational changes are brought about by the interaction between MBP and MalFGK<sub>2</sub>.

To address the question of whether the closed, unliganded form of the binding protein can stimulate ATP hydrolysis by the transporter, we engineered maltose binding protein so that the open conformation is destabilized relative to the closed conformation, and assayed the ability of these forms of the protein to activate the membrane-bound ATPase. In addition, we have carried out a careful analysis of the ability of unliganded MBP to stimulate the membrane ATPase, and demonstrate that the characteristics of this stimulation are completely different

from what is observed for ligand-bound MBP. The results we have obtained make it highly unlikely that, in the absence of maltose, a closed conformation of MBP is responsible for stimulation of MalFGK<sub>2</sub>, and we suggest instead that it is the more stable and abundant open conformation.

## MATERIALS AND METHODS

### Bacterial strains and plasmids

The bacterial strain HS3399 was used for expression for all transport complexes, and was originally derived from the parental strain of *Escherichia coli* K12 (24). This strain contains the  $\Delta malB101$  allele, a deletion of the entire *mal* operon, and the  $\Delta atp$  allele, a deletion of the gene for F<sub>1</sub>-ATPase. *E. coli* strain HS3309 (25) was used for expression of periplasmic MBP and MBP-DM from pLH1 (26) and pLH1-DM (27); HS3309 does not produce chromosomally encoded MBP and has constitutive expression of the maltose operon activator, MalT to drive expression from pLH1. In the MBP-DM mutant, residues 172, 173, 175, and 176 are deleted, resulting in a truncated surface loop, and M321 and Q325 are both mutated to alanine. The plasmid pNTSK+ contains *malF* and *malG* genes preceded by the IPTG-inducible pTac promoter. pNTSK+ was produced by digesting the plasmid pCP8 (24) with EcoRI to remove the tethered MBP expression cassette. Since this cassette also contained the ampicillin resistance marker, pBluescript II SK+ (Fermentas) was cloned into the EcoRI site to restore ampicillin resistance. pMR11, which is replicative-compatible with pNTSK+, harbors the *malK* gene preceded by the pTac promoter sequence, and contains a chloramphenicol resistance marker. pMal-96W329W contains the coding sequence for cytoplasmic MBP with the balancing interface mutations A96W and I329W (23).

**Construction of hexahistidine-tagged MBP**—To increase the efficiency of purification and the yield of MBP, the MBP coding sequence was cloned into pProEX-HTa (Invitrogen) for intracellular expression of a hexahistidine-tagged version of MBP connected by a TEV protease cleavable linker. Restriction sites for cutting and inserting EheI and HindIII were introduced into the pLH1 vectors by mutagenic PCR, with primers: 5' CGCCTCGGCTGGCGCCAAAATCGAAG-3' (forward) and 5' CGCCGCATCCGGCATTTAAGCTTATTACTTGGTGATACGAG-3' (reverse).

The entire MBP coding sequence was verified.

### Expression and purification of MBP

**Wild-Type MBP and MBP-DM**—All chromatographic media were purchased from GE Healthcare. Plasmids containing wild-type (pLH1) or mutant (pLH1-DM) *malE* coding regions were transformed into *E. coli* strain HS3309. Cultures were grown with vigorous shaking at 30 °C in LB broth containing 100 µg/mL ampicillin for 16 to 18 h. Periplasmic proteins were extracted by osmotic shock and dialyzed against 50 mM Tris-HCl, pH 8.5 in preparation for anion exchange chromatography. The extract was applied onto a 2.6 × 15 cm column packed with Q-Sepharose Fast Flow and eluted with a linear gradient from 0 to 1 M NaCl, with a base buffer of 50 mM Tris-HCl, pH 8.5. Fractions containing MBP were pooled and dialyzed against 50 mM Tris-HCl, pH 8.5. Depending on the purity of MBP containing fractions at this step, a further ion-exchange step using a Mono-Q column was sometimes necessary before moving on to the next step.

To effect further purification and remove contaminating maltose from preparations of MBP, protein from the ion exchange column(s) was diluted in 50 mM Tris-HCl, and dialyzed against two changes of a 100-fold excess 2 M guanidine hydrochloride. Guanidine hydrochloride was then slowly removed by dialysis against a four changes of a 100-fold excess of 50 mM Tris-

HCl pH 8.5. The refolded MBP was concentrated by ion-exchange chromatography using a 1-mL HiTrap Q column. Concentrated protein was loaded onto a 2.6 × 60 cm column of Superdex 200 Prep Grade gel filtration resin, which had been equilibrated with 20 mM Hepes, 100 mM KCl, pH 7.4. The column was developed with this same buffer at a flow rate of 0.5 mL/min. Fractions containing pure MBP were pooled and dialysed against 2 changes of a 100-fold excess of 50 mM Tris pH 8.0. MBP was concentrated on a 1 mL HiTrap Q column, and then dialyzed against a 100-fold excess of 50 mM Tris-HCl pH 7.0, 100 mM KCl, 10 mM MgCl<sub>2</sub>.

**MBP-A96W/I329W**—To express and purify the cytoplasmic MBP-A96W/I329W, HS3309 cells were transformed with pMal-A96W/I329W, and a single colony was used to inoculate 100 mL LB-Amp. This culture was grown with vigorous shaking to an optical density of 0.1 and 100  $\mu$ L was added to 1 L of LB-Amp. The culture was grown to an OD<sub>600</sub> of 0.4 and expression of MBPA96W/I329W was induced by addition of 100  $\mu$ g/mL IPTG and the culture grown for a further 6 hours at 37°C. Cells were ruptured by passage through a French Pressure cell at 20,000 p.s.i, and pure MBP was obtained by anion-exchange and gel filtration chromatography as described above.

**Histidine-Tagged MBP**—For later experiments involving stimulation of MalFGK<sub>2</sub> with high concentrations of MBP, the protein was expressed intracellularly in a BL21(DE3) background, as a fusion protein with a TEV protease cleavable hexahistidine tag. After growth, induction, and harvesting (as described for MBP-A96W/I329W, above) the cell pellet was resuspended in 50mL of Ni<sup>2+</sup>-NTA buffer (20mM Hepes, 500 mM KCl, 10 mM imidazole, 10% glycerol, pH 8.0) and supplemented with 1 mM PMSF before lysis by 3 passes through a French pressure cell at 20,000 psi. Cell debris was pelleted at 100,000 g and the supernatant applied to Ni<sup>2+</sup>-loaded Chelating Sepharose FF and proteins eluted using an imidazole gradient from 10 to 250 mM. High purity fractions containing MBP were pooled and a 1:20 mass ratio of TEV protease was added; the solution was dialyzed overnight at 4°C against 4L of Ni<sup>2+</sup>-NTA buffer to remove excess imidazole. The TEV protease treated protein was loaded onto clean Ni<sup>2+</sup>-NTA resin and MBP, with the histidine tag removed, was collected from the flow through. The cleaved MBP was dialyzed overnight against 4L of 50 mM Tris-HCl, pH 8.5, in preparation for anion exchange chromatography.

**Denaturation and refolding of MBP**—Fractions from the anion exchange column containing pure MBP were pooled and denatured by overnight dialysis against a 5-fold excess of 6 M guanidine-HCl. The denatured protein was subsequently dialyzed against 5 changes of a 10-fold excess of 6 M guanidine-HCl at 4°C, resulting in a ligand dilution of 500,000-fold; 5mM EDTA was included in the final 2 dialysis buffers. Protein was refolded by dialysis against 1 M guanidine-HCl, 5mM EDTA, and then dialyzed twice against a 50-fold excess of 50 mM Tris-HCl pH 8.5.

Note that the proper refolding and function of all MBP preparations was tested by fluorescence titrations with maltose and/or maltotriose: the refolded MBP preparations typically yielded a higher degree of fluorescence quenching due to complete removal of ligand. To maintain consistency between ATPase assays in both the absence and presence of maltose, all MBP preparations were subjected to the same unfolding and refolding procedure.

## Proteoliposomes

**Over-expression of MalFGK<sub>2</sub>**—HS3399 cells were co-transformed with plasmids carrying the malF and malG genes (pNTSK+), and the malK gene (pMR11). A single colony was inoculated into 100 mL of LB (containing 100  $\mu$ g/mL ampicillin, and 50  $\mu$ g/mL chloramphenicol), and grown to a OD<sub>600</sub> of 0.1; 100  $\mu$ L of this culture was added to each liter of the same media, and cells were grown with vigorous shaking at 37°C, to an OD<sub>600</sub> of 0.4;

expression of MalFGK<sub>2</sub> was induced by the addition of 100 µg/mL IPTG and grown for 8 hours at 37°C. The cell pellet from each liter was washed twice with 50 mL of 20 mM Hepes pH 7.0, and crude membranes were prepared as follows: each gram of washed cells was re-suspended in 10 mL of 20 mM Hepes 7.0, 5mM MgCl<sub>2</sub>, with 10% glycerol, and passed twice through a French pressure cell at 15,000 psi. Cell debris was removed by centrifugation at 7,000 g for 10 minutes. The supernatant was then subjected to ultracentrifugation at 100,000 g to recover membranes. Membranes were washed twice in 10 mM MOPS pH 7.5, 5mM MgCl<sub>2</sub>, 200 mM sucrose, and resuspended in 10 mM MOPS pH 7.5, 5mM MgCl<sub>2</sub>, 200 mM sucrose, with 10% methanol.

**Solubilization of membrane protein**—Washed membrane vesicles were recovered by centrifugation at 100,000 g and re-suspended at a protein concentration of 5 mg/mL in 50 mM Tris-HCl, pH 7.0, 1.2% β-octylglucoside, and 10 mM MgCl<sub>2</sub>. This solution was kept on ice with occasional agitation for 60 minutes, and was subsequently subjected to ultracentrifugation at 100,000 g for 45 minutes to pellet the insoluble material. The remaining supernatant containing the solubilized protein fraction was kept at 4°C until use.

**Preparation of PLS**—Crude *E. coli* phospholipids (Avanti Polar Lipids) were dissolved at a concentration of 50 mg/mL in chloroform. The chloroform was removed using a rotary evaporator, leaving a lipid film on the round bottom flask, and the lipids were re-hydrated with 50 mM Tris-HCl, pH 7.0, and 1 mM DTT at a concentration of 50 mg/mL. Lipid aliquots of 200 µL were quick-frozen, and stored under argon at -80°C until use. Lipid suspensions were thawed and sonicated to clarity using a microtip sonicator before the next step. To reconstitute the intact transporter into PLS, 450 µL of solubilized transporter (5 mg/mL) was mixed with 100 µL (50 mg/mL) of sonicated lipids, and kept on ice 30 minutes. PLS were then formed using the detergent dilution procedure (28) as follows: the protein/lipid solution was diluted slowly using a peristaltic pump with 50 mM Tris-HCl, pH 7.0, and 1 mM DTT to a volume of 20 mL. PLS were recovered by ultracentrifugation at 100,000 g for 45 minutes. PLS were then washed once using this same buffer and re-suspended in 500 µL. Total protein determination was done using the Lowry method. Typically PLS solutions were at a final protein concentration of approximately 2 mg/mL.

### Assay of ATPase activity

PLS were added to yield a final concentration of 0.1 mg/mL in 50 mM Tris-HCl pH 8.0, 100 mM KCl, 10 mM MgCl<sub>2</sub> in a total volume of 750 µL. Purified MBP was added with and without 5 mM maltose. The reaction was started by the addition of 750 µL of 50 mM Tris-HCl, 8 mM ATP, 10 mM MgCl<sub>2</sub>, pH 8.0. Aliquots of 300 µL were removed at 0, 5, 10, 20 and 30 minute time intervals and added to 150 µL of 10% SDS to stop the reaction and disrupt the PLS. The amount of free phosphate liberated during the reaction was then monitored by adding 250 µL color reagent (10 mM ammonium molybdate and 1 mM FeSO<sub>4</sub> in 1 N H<sub>2</sub>SO<sub>4</sub>) and measuring the absorbance at 740 nM. Standard solutions of potassium phosphate were measured using the same reagents to produce a standard phosphate curve. To conserve binding proteins and liposomes, we also used a 5-fold scaled-down version of the assay with a final volume of 360 µL rather than the 1.5 mL described above. In this case, PLS and MBP were mixed in a volume of 342 µL, and the reaction was initiated with 18 µL of 80 mM ATP, 50 mM Tris-HCl, 100 mM KCl, pH 8.0. Aliquots of 60 µL were removed at 0, 5, 10, 20, and 30 minutes and mixed with 30 µL 10% SDS, followed by 50 µL of color reagent.

### CD Spectroscopy

Thermal denaturation of wild-type and mutant MBP molecules was monitored using a JASCO J715A spectropolarimeter. Proteins were dialyzed against 10 mM sodium phosphate, pH 7.4, with or without 500 µM maltose. Buffer scans were acquired under similar conditions. A

thermal melt was carried out with the refolded proteins in a 0.1 cm path length quartz cuvette by monitoring the CD signal at 222 nm. The sample was heated from 20 to 95 °C with a heating rate of 75 °C/h using a JASCO PTC-348WI Peltier device. A bandwidth of 0.2 nm and a response time of 4 s were used. Transition points were determined by linear extrapolation of the plateau regions using the following equation (29):

$$y = \frac{(y_n + m_n x) + (y_u + m_u x) \exp \left[ \frac{\Delta H_m}{R} \left( \frac{1}{T_m} - \frac{1}{x} \right) \right]}{1 + \exp \left[ \frac{\Delta H_m}{R} \left( \frac{1}{T_m} - \frac{1}{x} \right) \right]} \quad (1)$$

In this expression  $x$  is the temperature in degrees Kelvin;  $y_n$  and  $y_u$  refer to the molar ellipticity of the folded and unfolded plateaus, respectively;  $m_n$  and  $m_u$  are the slopes of the plateaus;  $R$  is the universal gas constant in units of kcal•mol<sup>-1</sup>•K<sup>-1</sup>;  $T_m$  is the melting temperature in degrees Kelvin; and  $\Delta H_m$  is the enthalpy of unfolding at  $T_m$  in kcal•mol<sup>-1</sup>. Thermal denaturation of MBP is largely irreversible and therefore the fitted  $T_m$  and  $\Delta H_m$  values lack quantitative thermodynamic significance, but are useful for a semi-quantitative comparison of thermal denaturation in the presence and absence of maltose.

### Small Angle X-ray Scattering

SAXS experiments were carried out at BioCAT beamline ID18 at the Advanced Photon Source (Argonne Illinois, U.S.A.) essentially as described previously (30). Radii of gyration were calculated with the program *GNOM* (31) and *CRY SOL* (32) was used for matching crystal structures to SAXS data.

### Modelling of MBP-Dependent ATPase Kinetics

Steady state and mass balance equations were created based on the kinetic models illustrated in Figure 4. In these schemes, BPo and BPC represent open and closed MBP, respectively, and BPoM and BPCM are the corresponding complexes between MBP and MalFGK<sub>2</sub>. For each of the kinetic models, the equations were solved analytically, providing the steady state concentration of the “active” complex in terms of the total amount of binding protein and membrane complex, plus the rate constants. The rate constants are only relative values: they were initially set at 1 and then adjusted to reflect the observed properties of the system.

For the case where only the closed form of MBP stimulates ATP hydrolysis (Figure 4A), equations 2 to 6 were used:

$$[M_T] = [M] + [BPoM] + [BPCM] \quad (2)$$

$$[BP_T] = [BPo] + [BPC] \quad (3)$$

$$k_3 [BPo] = k_{-3} [BPC] \quad (4)$$

$$\frac{d[BPoM]}{dt} = 0 = k_1 [BPo][M] + [BPCM](k_{-4} + k_{cat}) - [BPoM](k_{-1} + k_4) \quad (5)$$

$$\frac{d[\text{BPcM}]}{dt}=0=k_2[\text{BPC}][\text{M}]+k_4[\text{BPoM}]-[\text{BPcM}](k_{-2}+k_{-4}+k_{cat}) \quad (6)$$

For simplicity, the equations incorporate the following assumptions: first, the membrane-bound binding protein represents a relatively small proportion of the total, and therefore membrane-bound forms are not included in the mass balance equation for total binding protein (equation 3); second, the open and closed forms of the free binding protein are assumed to be in equilibrium (equation 4).

For the case that includes the presence of an alternate conformation of the membrane complex (denoted by  $M^*$ ) and activation by open MBP (Figure 4B), equations 6 to 10 were used. Here we assumed that the proportion of the activated form of the membrane complex ( $M^*$  and  $\text{BPoM}^*$ ) was relatively small, and was therefore not included in the mass balance equation for the membrane complex (equation 7). Furthermore, all of the binding protein is assumed to be in the open, free form (equation 8).

$$[M_T]=[M]+[\text{BPoM}] \quad (7)$$

$$[\text{BP}_T]=[\text{BPo}] \quad (8)$$

$$\frac{d[M^*]}{dt}=0=k_3[M]+k_{-2}[\text{BPoM}^*]-k_{-3}[M^*]-k_2[M^*][\text{BPo}] \quad (9)$$

$$\frac{d[\text{BPoM}]}{dt}=0=k_1[\text{BPo}][M]+[\text{BPoM}^*](k_{-4}+k_{cat})-[\text{BPoM}](k_{-1}+k_4) \quad (10)$$

$$\frac{d[\text{BPoM}^*]}{dt}=0=k_2[\text{BPo}][M^*]+k_4[\text{BPoM}]-[\text{BPoM}^*](k_{-2}+k_{-4}+k_{cat}) \quad (11)$$

## RESULTS

### Stimulation of the MalFGK<sub>2</sub> ATPase by MBP

We investigated the roles of MBP and maltose in stimulation of the MalFGK<sub>2</sub> ATPase using a proteoliposome (PLS) system. MalFGK<sub>2</sub> was over-expressed and PLS were formed from cell membranes by a detergent dilution procedure. After detergent dilution, MalFGK<sub>2</sub> will be present in both orientations in the PLS bilayer. A high concentration of  $\text{Mg}^{2+}$  was used to promote membrane fusion and mixing; therefore, fixed, closed vesicles do not exist in this system, allowing for bi-directional maltose transport (33). Importantly, the same PLS preparation can be reconstituted with varying concentrations of MBP or MBP mutants, thereby controlling for differences in the amount and specific activity of MalFGK<sub>2</sub> in the membranes.

The presence of MalF, MalG, and MalK in the PLS was confirmed by Western blotting (not shown). The PLS on their own had a basal ATPase that represents uncoupled activity from

MalFGK<sub>2</sub> and/or other soluble or membrane-bound ATPases. Regarding the preparation of MBP, we found that when MBP is purified from a periplasmic extract, it co-purifies with a contaminating ATPase; in addition, MBP tends to retain some maltose, even after several purification steps. Contamination of MBP with an ATPase and/or maltose can confound the ATPase measurements and preclude accurate comparisons between the effect of unliganded and maltose-bound MBP on the MalFGK<sub>2</sub> ATPase. We addressed these problems by intracellular expression of MBP as a hexa-histidine tagged fusion protein. After initial purification by Ni<sup>2+</sup>-NTA chromatography and cleavage of the tag, leaving only two extra residues (glycine and alanine) at the N-terminus, MBP was purified by ion-exchange chromatography yielding a single band by SDS-PAGE with no significant contaminating ATPase activity. To ensure that it was totally free of maltodextrins, the MBP was fully denatured, dialyzed exhaustively against 6 M guanidine-HCl, and then refolded. Proper refolding and function of MBP preparations was confirmed by fluorescence titration with maltose and/or maltotriose.

Unliganded MBP prepared in this manner was used for all assays, with or without maltose. Unliganded MBP (2 μM) stimulated the ATPase activity by approximately 50% at 20°C and 100% at 37°C (Figure 1). As discussed, the MBP preparation that was added to the PLS had no significant ATPase activity on its own, and had been fully denatured, dialyzed, and refolded to ensure that absolutely no maltose was present. Therefore the stimulation was due solely to an interaction between unliganded MBP and MalFGK<sub>2</sub>. These results, including the ability of unliganded MBP to stimulate MalFGK<sub>2</sub>, are similar to what was observed previously for the maltose transport system (4), and a significant stimulation by the unliganded binding protein has also been documented for the histidine transporter (5).

### Concentration dependence of MBP-mediated MalFGK<sub>2</sub> stimulation

To further characterize the activation of the MalFGK<sub>2</sub> ATPase by both unliganded and liganded MBP, we studied the effect of changing the MBP concentration at both 20° and 37°C. In the presence of maltose, increases in MBP concentration led to almost proportional increases in ATPase activity that began to reach a plateau at 10 μM, presumably as membrane-bound MalFGK<sub>2</sub> became saturated with maltose-MBP. In this respect the system resembles a single substrate enzyme, where MalFGK<sub>2</sub> is the enzyme and MBP-maltose is the substrate. The ATPase rate versus MBP concentration data were fit to a simple Michaelis-Menten equation, yielding a  $K_M$  of approximately 15 μM (defined as the concentration of MBP-maltose that yields one half  $V_{MAX}$ ) at both 20° and 37°, and  $V_{MAX}$  values of 1400 and 5500 nmol•mg<sup>-1</sup>•min<sup>-1</sup> at 20° and 37°C respectively (Table 1 and Figure 2).

The same experiments were carried out with MBP that was completely free of maltose. At 20° C, addition of unliganded MBP at concentrations of 2 μM and 20 μM produced exactly the same modest increase in ATPase activity (Figure 3A). This is in contrast to the situation for maltose-bound MBP, in which a similar 10-fold increase in concentration produced close to a 10-fold increase in activity (Figure 2A). Increasing unliganded MBP concentration from 1 to 100 μM produced no significant increase in the stimulation of MalFGK<sub>2</sub> ATPase (Figure 3B). When these data were fit to a Michaelis-Menten equation, the calculated  $K_M$  was 0.6 μM, over 20-fold lower than the  $K_M$  for liganded MBP. We also carried out the assays at 37°C where the stimulation by unliganded MBP was greater, allowing us to obtain rate data at concentrations of unliganded MBP lower than 1 μM. At 37°C, increasing the unliganded MBP concentration from 0.1 through to 100 μM produced only a modest increase in the activation of MalFGK<sub>2</sub>, with a calculated  $K_M$  of 0.8 μM (Figure 2C and Table 1), almost 20-fold lower than the  $K_M$  obtained for maltose-bound MBP at 37°C.



### Kinetic models for stimulation of the MalFGK<sub>2</sub> ATPase by unliganded MBP

Unliganded MBP must stimulate the MalFGK<sub>2</sub> ATPase through either its closed or open conformation. To investigate in more detail the expected MBP concentration dependence for these two possibilities, we modeled the kinetics of the activation process. A potential complicating factor is the “passive” (i.e. non-activating) interaction between unliganded MBP and MalFGK<sub>2</sub> which was first postulated on a theoretical basis and then observed experimentally (34,35). We incorporated this interaction into two models for the stimulation of the MalFGK<sub>2</sub> ATPase by unliganded MBP. The relative affinity of the open conformation is approximately 3-fold less than the closed form (Figure 4A and Table 2;  $k_{-1}/k_1 = 50$ ,  $k_{-2}/k_2 = 15$ ), which is based on mathematical modeling of the system as well as the measured affinities of open and closed MBP for the isolated MalF P2 loop (16,35,36).

In the first model (Figure 4A), MBP alternates between open and closed conformations with both forms binding to MalFGK<sub>2</sub>, but only the closed form stimulating ATP hydrolysis. To test the model, we used it to predict what would be observed in the presence of saturating maltose. For this, MBP will be present only in the closed, liganded form, which can be accomplished in the model by making the rate constants for the closed to open transition of MBP ( $k_{-3}$  and  $k_4$ ) very small (Figure 4A and Table 2). With this set of rate constants, the system produces the observed  $K_M$  of 15  $\mu\text{M}$  (Figure 5A); from the modeling, we obtain a relative concentration of the “active” species (in this case, liganded MBP bound to MalFGK<sub>2</sub>), which can vary from 0 to 1; we applied a factor to obtain a  $V_{\text{max}}$  close to the 5500  $\text{nmol}\cdot\text{min}^{-1}\cdot\text{mg}^{-1}$  we observed experimentally. The situation in the absence of maltose is similar, except that  $k_{-3}$  and  $k_4$  are made larger to reflect the shift towards the open conformation of binding protein (Table 2); the value of 10 was chosen for both  $k_{-3}$  and  $k_4$  so that the rate of ATP hydrolysis at 1 or 2  $\mu\text{M}$  unliganded MBP compared well with what was observed experimentally. If the system operated through this mechanism in the absence of maltose, then the apparent  $K_M$  for MBP would be just over 40  $\mu\text{M}$ , and there would be a 15-fold increase in the MalFGK<sub>2</sub> ATPase activity as the MBP concentration was raised from 1  $\mu\text{M}$  to 25  $\mu\text{M}$  (Figure 5B). We attempted to improve the agreement with experimental data by using different parameter sets, but found that the only way to lower the  $K_M$  for MBP was to increase the affinity of the interaction between MalFGK<sub>2</sub> and open MBP (i.e. decrease  $k_{-1}$ ) such that it is at least 20-fold higher than the affinity of the interaction between MalFGK<sub>2</sub> and closed MBP. Such parameters are at odds with the relatively weak ability of unliganded MBP to inhibit transport by liganded MBP (35) as well as direct binding measurements between MBP and the isolated P2 loop of MalF (36).

The alternative mechanism in which the open conformation of MBP stimulates the MalFGK<sub>2</sub> ATPase provides a better fit to the observed data. In this model (Figure 4B and Table 2 for parameter values), only open unliganded MBP is present and it has the same passive interaction with MalFGK<sub>2</sub> as in the previous model. However, there is a second form of MalFGK<sub>2</sub>, “M\*”, which is able to bind open unliganded MBP with high affinity (note the low value of  $k_{-2}$  in Table 2), producing the transition state complex, leading to ATP hydrolysis and regeneration of MalFGK<sub>2</sub> to its “resting” conformation. In addition to the low rate of dissociation of the transition state complex, there is a low rate of formation of M\*, which limits the maximum rate of catalysis. The low rate constants for the formation of M\* ( $k_3$  and  $k_4$ ), as well as the low rate constant for dissociation of the transition state complex ( $k_{-2}$ ) lead to behaviour that is close to what was observed, namely a  $K_M$  of  $\sim 1 \mu\text{M}$  and low  $V_{\text{MAX}}$ . The  $K_M$  can be lowered further, to sub-micromolar levels, by slowing the rate of conversion of M\* to M (decreasing constants  $k_{-3}$  and  $k_{-4}$ ; Table 2 and Figure 5B).

In summary, unliganded MBP stimulates the MalFGK<sub>2</sub> ATPase with a  $K_M$  below 1  $\mu\text{M}$ , and the nature of the stimulation is not consistent with a mechanism in which a minor species adopts a closed, unliganded conformation to mimic the effect of closed, liganded MBP. Instead, the

stimulation is consistent with a small amount of MalFGK<sub>2</sub> crossing an energetic barrier to adopt an alternate conformation to which open MBP binds with high affinity, leading to ATP hydrolysis in the absence of maltose.

### Conformational engineering of MBP

To further address the roles of the open and closed conformations of MBP, we used “conformationally-engineered” MBP molecules in which the open conformation is selectively destabilized relative to the closed conformation. Selective destabilization of the open conformation will shift the open-closed equilibrium of unliganded MBP towards the closed conformation. On this basis, if it is the closed conformation of unliganded MBP that stimulates MalFGK<sub>2</sub>, then the shift in the open-closed equilibrium should result in a greater stimulation of MalFGK<sub>2</sub> in the absence of maltose.

Selective destabilization of the open conformation was accomplished by altering residues in a region we have called the “balancing interface”. MBP is composed of two globular domains connected by a flexible hinge: the maltose binding cleft is on one side of the hinge, and the balancing interface is on the opposite side, where it balances or counteracts closing of the maltose-binding cleft. One of the conformationally-engineered MBP molecules, MBP-DM, had been mutated to remove favorable interactions in the balancing interface that stabilize the open conformation (27). Crystal structures and small angle X-ray scattering (SAXS) of MBP-DM indicated that it adopts exactly the same open and closed conformations as wild-type MBP; however, its maltose affinity is approximately 100 times higher than wild-type due to selective destabilization of the open, unliganded conformation.

Other groups have destabilized the open conformation by replacement of balancing interface residues with bulkier substituents (23,37). One such mutant, MBP-A96W/I329W, has an average solution conformation corresponding to a domain closure of 28° (23), which is close to the 35° domain closure in maltose-bound MBP. We used SAXS to further verify the perturbed solution conformation of MBP-A96W/I329W. Addition of maltose to ligand-free MBP-A96W/I329W resulted in a barely detectable change in the radius of gyration from 22.2 Å for the unliganded protein, to 22.1 Å for the maltose-bound protein (Figure 6A). When compared to crystal structures for wild-type MBP, the solution conformation of MBP-A96W/I329W most closely resembles the closed maltose-bound structure of MBP (Figure 6B). As with MBP-DM, the affinity of MBP-A96W/I329W for maltose is much higher than that of wild-type MBP, consistent with selective destabilization of the open conformation. On this basis, and assuming that the wild-type protein exists to some degree in a closed, unliganded conformation in solution, both of the mutant MBPs are expected to sample a closed unliganded conformation more frequently than wild-type MBP.

The selective destabilization of the open, unliganded conformations of MBP-DM and MBP-A96W/I329W can be seen from thermal denaturation curves (Figure 7): in the presence of maltose the T<sub>m</sub> values for wild-type MBP, MBP-DM, and MBP-A96W/I329W were similar (65°C for wild-type versus approximately 64°C for the two mutants) whereas in the absence of maltose the T<sub>m</sub> values for MBP-DM and MBP-A96W/I329W were both significantly decreased (to 53 °C) compared to unliganded wild-type MBP (63 °C). The mutations in MBP-DM and MBP-A96W/I329W are not directly involved in ligand binding; furthermore, since they are on the opposite side of the protein from where MBP and MalFGK<sub>2</sub> interact, they will not directly interfere with binding to MalFGK<sub>2</sub> (11,25,26) and the mutations should not affect the structure of any closed, unliganded conformations that may exist in solution. A productive interaction between these mutants and MalFGK<sub>2</sub> is demonstrated by the fact that they both support growth on maltose minimal media in an MBP-deficient strain (not shown). For the purposes of these experiments, therefore, the closed, maltose-bound forms of MBP-DM and

MBP-A96W/I329W are identical to wild-type, but the open conformations have been destabilized.

To explore the importance of the open and closed conformations of MBP in maltose transport, we compared the ability of wild-type MBP and MBP-DM to stimulate the MalFGK<sub>2</sub> ATPase in both the presence and absence of maltose (Figure 8). In the absence of maltose, MBP-DM stimulated ATP hydrolysis to the same degree as wild-type. Therefore, shifting the open-closed equilibrium of MBP towards the closed conformation does not enhance the ability of MBP to stimulate MalFGK<sub>2</sub> in the absence of maltose, as would be expected if it were the closed conformation that is responsible for the stimulation. Surprisingly, in the presence of maltose MBP-DM was significantly impaired its ability to stimulate MalFGK<sub>2</sub> compared to wild-type MBP. This was an unexpected result because the mutations only affect the stability, and not the structure, of the open conformation. Open MBP forms a tight transition state complex with MalFGK<sub>2</sub> (11,17) and these kinetics results show that the balancing interface of MBP contributes to ATP hydrolysis, probably by enhancing the stability of the transition state complex.

The results obtained with MBP-DM were reinforced by experiments with MBP-A96W/I329W (Figure 8). In the absence of maltose, stimulation of MalFGK<sub>2</sub> by MBP-A96W/I329W was not significant, and in fact the mutations have decreased and possibly abrogated its ability to stimulate MalFGK<sub>2</sub> in the absence of maltose. Given that unliganded MBP-A96W/I329W adopts an average conformation that is almost closed, the inability of unliganded MBP-A96W/I329W to stimulate MalFGK<sub>2</sub> is not consistent with the idea that the closed conformation alone is responsible for stimulation in the absence of maltose. Addition of maltose to MBP-A96W/I329W brought about a significant stimulation of the MalFGK<sub>2</sub> ATPase, although it was much less than stimulation by wild-type MBP. These measurements were made at an MBP concentration of 2  $\mu$ M, but the same results were obtained at 1  $\mu$ M and 5  $\mu$ M MBP concentrations (not shown): in the presence of maltose, increases in the concentration of all three proteins produced increases in stimulation of the MalFGK<sub>2</sub> ATPase, but MBP-DM consistently exhibited a modestly compromised ability to stimulate MalFGK<sub>2</sub> compared to wild-type MBP, while MBP-A96W/I329W was severely compromised.

Thus, mutations destabilizing the open conformation do not enhance the ability of the proteins to stimulate the MalFGK<sub>2</sub> ATPase in the absence of maltose, and in fact reduce the maltose-stimulated MalFGK<sub>2</sub> ATPase activity. In this regard, we have considered the possibility that decreases in the ability of the mutants to stabilize the transition state might have offset increased stimulation by higher proportions of the closed conformation. We believe this is highly unlikely. Both of the mutants have ligand binding affinities that are at least 2 orders of magnitude higher than wild type, and on this basis the open-closed equilibrium has been severely perturbed. Assuming the destabilizing mutations have the same effect on the unliganded protein as they do on the ligand-bound protein, then one would expect a significant (up to 2 orders of magnitude) increase in the fraction of closed unliganded MBP in solution. In contrast, destabilization of the open conformation produces only a modest 20% decrease in maltose-stimulated ATPase activity for MBP-DM, and a 5-fold decrease for MBP-A96W/I329W. Therefore it is unlikely that increases in the proportion of the closed conformation of these mutants - and associated increases in MalFGK<sub>2</sub> stimulation - are being completely masked or offset by their decreased ability to stabilize the transition state.

In summary, the closed conformation is most likely not responsible for stimulation of the ATPase in the absence of maltose. In addition, the results with the conformationally engineered MBP mutants show that the energetics of domain opening, and the stability of the open conformation, are important for ATP hydrolysis.

## DISCUSSION

The mechanism of substrate import by ABC import systems involves binding of ligand to the peripheral binding protein to exert a conformational change that signals to the integral membrane subunits to initiate ATP hydrolysis. The shape complementarity of the interacting surfaces - closed MBP and an undefined conformation of MalFGK<sub>2</sub> - is critical, and this has been demonstrated through mutagenic studies (25,26). Along with many other peripheral binding proteins, unliganded MBP exists in an open conformation in solution (15,38–40), and therefore it has always been difficult to understand how the unliganded binding protein is able to stimulate ATP hydrolysis by the transporter, an effect documented for the two systems that have been tested in this regard - the maltose and histidine transporters (4,5). One possible explanation is that the unliganded binding protein is able to mimic the closed conformation of the protein. In other words, the system follows a “lock and key” model: as long as the binding protein has the correct shape, it should be able to activate the MalFGK<sub>2</sub> ATPase. Evidence for a closed, unliganded conformation includes crystallization of the glucose/galactose binding protein in an unliganded, closed conformation (19), and, more recently, the ChoX protein from *S. meliloti* (20). In addition, an alternate solution conformation for the maltose binding protein (MBP) has been documented by NMR (18) and in solution the overall conformation of unliganded MBP appears to be slightly more closed than the unliganded crystal structure (15, 27) hinting that MBP may exist, to some degree, in closed conformation(s) in solution. Apart from these results, which are consistent with the existence of a small fraction of a closed, unliganded form of the binding protein in solution, there is no experimental evidence for the stimulation of the membrane ATPase by a closed, unliganded conformation of the binding protein. The idea is based solely on the fact that the closed, liganded form is responsible for stimulation in the presence of ligand.

This study was initiated to test whether activation of the MalFGK<sub>2</sub> ATPase by unliganded MBP was due to a closed unliganded conformation. Our hope was that this information would help us to understand the molecular mechanics of the system, and, more specifically, to address the role of maltose itself in the transport process. Our results argue against the idea that unliganded MBP stimulates the transporter through a closed conformation. The dependence of the stimulation on MBP concentration does not follow what would be expected if this were the mechanism. Specifically, the unliganded form of the protein stimulates MalFGK<sub>2</sub> with a much lower  $K_M$  value than maltose-bound MBP, indicating that the species responsible is not mimicking the closed conformation of MBP. Furthermore, destabilization of the open conformation - and consequent increase in the proportion of the closed conformation - had no positive effect on the ability of unliganded MBP to stimulate the MalFGK<sub>2</sub> ATPase.

We conclude that a closed, unliganded conformation of MBP is not responsible for MBP-dependent MalFGK<sub>2</sub> stimulation in the absence of maltose. One explanation for why this is the case is that ligand is required to stabilize the closed conformation of the binding protein. Much of the experimental work on the maltose transporter is consistent with the existence of energetic barriers to conformational changes in MalFGK<sub>2</sub> (41). These would represent higher energy intermediates of MalFGK<sub>2</sub> that prevent futile cycling and ATP hydrolysis in the absence of maltose. MBP may function to stabilize such intermediates, thereby promoting conformational changes in the system. However, to stabilize a high-energy MalFGK<sub>2</sub> intermediate, MBP would not only have to be in the correct conformation, but it would also have to be in a low energy state; that is, a high energy form of MBP would not contribute to the stabilization of a high energy form of MalFGK<sub>2</sub>. While the closed, liganded conformation represents a stable, low energy form of MBP, a closed unliganded conformation is an unstable high energy form (23), and on this basis, only ligand-bound MBP would be a good candidate for stabilizing a high energy form of MalFGK<sub>2</sub>.

The activation of the MalFGK<sub>2</sub> ATPase by unliganded MBP is most likely due to a high affinity interaction between the open conformation of MBP and a sparsely populated MalFGK<sub>2</sub> conformation. The maximum rate of ATP hydrolysis in the absence of maltose would be limited by the population of MalFGK<sub>2</sub> that is in the required conformation. MalFGK<sub>2</sub> has been crystallized in two conformational states (11,12), and in the membrane there may be other intermediates. At equilibrium the proportion of these different conformations will be determined by their relative energies, and there may also be kinetic barriers to interconversion between conformations. In either case, given finite limits on the energies of the conformations and kinetic barriers, a small proportion of the MalFGK<sub>2</sub> population will find itself in higher energy states, and these are the molecules to which open MBP could bind, promoting the ATPase activity by stabilizing the transition state or something close to it. The open, unliganded conformation is the second “low energy” form of MBP (after the closed, liganded conformation), and therefore would be able to stabilize a higher energy conformation of MalFGK<sub>2</sub>. We have demonstrated that destabilization of the open MBP conformation results in a decreased ability of MBP to stimulate the MalFGK<sub>2</sub> ATPase, consistent with the idea that the open conformation of MBP contributes to the stability of the transition state complex (11).

In addition to being consistent with the observations in this study, the idea of direct kinetic stabilization of a high energy form of MalFGK<sub>2</sub> by open MBP explains an observation made by Merino and Shuman (42). In this study, a MalFGK<sub>2</sub> mutant was isolated that was able to transport lactose, but only in the presence of MBP, which does not bind lactose. This work confirmed the importance of the interaction between unliganded MBP and the membrane components. Furthermore, given its robust stimulation of lactose transport and the fact that the vast majority of unliganded MBP is in an open conformation, it is almost certainly the open conformation of MBP that is required for lactose transport in this system.

## Acknowledgments

This research was supported by a Natural Sciences and Engineering Research Council Discovery Grant to BHS and Ontario Graduate Scholarship to PGT; ADG is the recipient of a Schulich Graduate Enhancement Scholarship. Use of Western’s Biomolecular Interactions and Conformations Facility was supported by the Schulich School of Medicine and Dentistry. Use of the Advanced Photon Source was supported by the United States Department of Energy, Basic Energy Sciences, Office of Science, under contract W-31-109-ENG-38 and BioCAT is supported by National Institutes of Health Research Grant RR-08630.

## ABBREVIATIONS

ABC	ATP Binding Cassette
MBP	maltose binding protein
PLS	proteoliposomes
SAXS	small angle X-ray scattering

## References

1. Higgins CF, Linton KJ. The ATP switch model for ABC transporters. *Nat Struct Mol Biol* 2004;11:918–926. [PubMed: 15452563]
2. Sauna ZE, Ambudkar SV. About a switch: how P-glycoprotein (ABCB1) harnesses the energy of ATP binding and hydrolysis to do mechanical work. *Mol Cancer Ther* 2007;6:13–23. [PubMed: 17237262]
3. Tomblin G, Senior AE. The occluded nucleotide conformation of p-glycoprotein. *J Bioenerg Biomembr* 2005;37:497–500. [PubMed: 16691489]

4. Davidson A, Shuman H, Nikaïdo H. Mechanism of maltose transport in *Escherichia coli*: Transmembrane signaling by periplasmic binding proteins. *Proc Natl Acad Sci USA* 1992;89:2360–2364. [PubMed: 1549599]
5. Ames GF, Liu CE, Joshi AK, Nikaïdo K. Liganded and unliganded receptors interact with equal affinity with the membrane complex of periplasmic permeases, a subfamily of traffic ATPases. *J Biol Chem* 1996;271:14264–1470. [PubMed: 8662800]
6. Borths EL, Poolman B, Hvorup RN, Locher KP, Rees DC. In vitro functional characterization of BtuCD-F, the *Escherichia coli* ABC transporter for vitamin B12 uptake. *Biochemistry* 2005;44:16301–16309. [PubMed: 16331991]
7. Chen J, Lu G, Lin J, Davidson AL, Quioco FA. A tweezers-like motion of the ATP-binding cassette dimer in an ABC transport cycle. *Mol Cell* 2003;12:651–661. [PubMed: 14527411]
8. Lu G, Westbrooks JM, Davidson AL, Chen J. ATP hydrolysis is required to reset the ATP-binding cassette dimer into the resting-state conformation. *Proc Natl Acad Sci U S A* 2005;102:17969–17974. [PubMed: 16326809]
9. Daus ML, Landmesser H, Schlosser A, Muller P, Herrmann A, Schneider E. ATP induces conformational changes of periplasmic loop regions of the maltose ATP-binding cassette transporter. *J Biol Chem* 2006;281:3856–3865. [PubMed: 16352608]
10. Daus ML, Grote M, Müller P, Doebber M, Herrmann A, Steinhoff HJ, Dassa E, Schneider E. ATP-driven MalK dimer closure and reopening and conformational changes of the “EAA” motifs are crucial for function of the maltose ATP-binding cassette transporter (MalFGK2). *J Biol Chem* 2007;282:22387–22396. [PubMed: 17545154]
11. Oldham ML, Khare D, Quioco FA, Davidson AL, Chen J. Crystal structure of a catalytic intermediate of the maltose transporter. *Nature* 2007;450:515–521. [PubMed: 18033289]
12. Khare D, Oldham ML, Orelle C, Davidson AL, Chen J. Alternating access in maltose transporter mediated by rigid-body rotations. *Mol Cell* 2009;33:528–536. [PubMed: 19250913]
13. Quioco FA, Ledvina PS. Atomic structure and specificity of bacterial periplasmic receptors for active transport and chemotaxis: variation of common themes. *Mol Microbiol* 1996;20:17–25. [PubMed: 8861200]
14. Bishop L, Agbayani R, Ambudkar SV, Maloney PC, Ames GF. Reconstitution of a bacterial periplasmic permease in proteoliposomes and demonstration of ATP hydrolysis concomitant with transport. *Proc Natl Acad Sci U S A* 1989;86:6953–6957. [PubMed: 2674940]
15. Evenäs J, Tugarinov V, Skrynnikov NR, Goto NK, Muhandiram R, Kay LE. Ligand-induced structural changes to maltodextrin-binding protein as studied by solution NMR spectroscopy. *J Mol Biol* 2001;309:961–74. [PubMed: 11399072]
16. Shilton B, Mowbray S. Simple Models for the Analysis of Binding Protein- dependent Transport Systems. *Protein Sci* 1995;4:1346–1355. [PubMed: 7670377]
17. Austeruhle MI, Hall JA, Klug CS, Davidson AL. Maltose-binding protein is open in the catalytic transition state for ATP hydrolysis during maltose transport. *J Biol Chem* 2004;279:28243–50. Epub 2004 Apr 26. [PubMed: 15117946]
18. Tang C, Schwieters CD, Clore GM. Open-to-closed transition in apo maltose-binding protein observed by paramagnetic NMR. *Nature* 2007;449:1078–1082. [PubMed: 17960247]
19. Flocco M, Mowbray S. The 1.9 Å X-ray Structure of a Closed Unliganded Form of the Periplasmic Glucose/Galactose Receptor from *Salmonella typhimurium*\*. *J Biol Chem* 1994;269:8931–8936. [PubMed: 8132630]
20. Oswald C, Smits SHJ, Hoing M, Sohn-Bosser L, Dupont L, Le Rudulier D, Schmitt L, Bremer E. Crystal Structures of the Choline/Acetylcholine Substrate-binding Protein ChoX from *Sinorhizobium meliloti* in the Liganded and Unliganded-Closed States. *Journal of Biological Chemistry* 2008;283:32848. [PubMed: 18779321]
21. Döring K, Surrey T, Nollert P, Jahnig F. Effects of ligand binding on the internal dynamics of maltose-binding protein. *Eur J Biochem* 1999;266:477–83. [PubMed: 10561588]
22. Stockner T, Vogel HJ, Tieleman DP. A salt-bridge motif involved in ligand binding and large-scale domain motions of the maltose-binding protein. *Biophys J* 2005;89:3362–3371. [PubMed: 16143635]

23. Millet O, Hudson RP, Kay LE. The energetic cost of domain reorientation in maltose-binding protein as studied by NMR and fluorescence spectroscopy. *Proc Natl Acad Sci U S A* 2003;100:12700–12705. [PubMed: 14530390]
24. Panagiotidis CH, Reyes M, Sievertsen A, Boos W, Shuman HA. Characterization of the structural requirements for assembly and nucleotide binding of an ATP-binding cassette transporter. The maltose transport system of *Escherichia coli*. *J Biol Chem* 1993;268:23685–23696. [PubMed: 8226895]
25. Treptow N, Shuman H. Allele-specific malE Mutations that Restore Interactions Between Maltose-binding Protein and the Inner-membrane Components of the Maltose Transport System. *J Mol Biol* 1988;202:809–822. [PubMed: 3050132]
26. Hor L, Shuman H. Genetic Analysis of Periplasmic Binding Protein Dependent Transport in *E. coli*: Each lobe of maltose-binding protein interacts with a different subunit of the MalFGK2 membrane transport complex. *J Mol Biol* 1993;233:659–670. [PubMed: 8411172]
27. Telmer PG, Shilton BH. Insights into the conformational equilibria of maltose-binding protein by analysis of high affinity mutants. *J Biol Chem* 2003;278:34555–34567. [PubMed: 12794084]
28. Davidson A, Nikaido H. Overproduction, Solubilization, and Reconstitution of the Maltose Transport System from *Escherichia coli*. *J Biol Chem* 1990;265:4254–4260. [PubMed: 2155217]
29. Swint L, Robertson AD. Thermodynamics of unfolding for turkey ovomucoid third domain: thermal and chemical denaturation. *Protein Sci* 1993;2:2037–2049. [PubMed: 8298454]
30. Telmer PG, Shilton BH. Structural studies of an engineered zinc biosensor reveal an unanticipated mode of zinc binding. *J Mol Biol* 2005;354:829–840. [PubMed: 16288781]
31. Semenyuk A, Svergun D. GNOM - a program package for small-angle scattering data processing. *J Appl Cryst* 1991;24:537–540.
32. Svergun D, Barberato C, Koch M. CRY SOL - a Program to Evaluate X-ray Solution Scattering of Biological Macromolecules from Atomic Coordinates. *J App Cryst* 1995;28:768–773.
33. Liu CE, Liu PQ, Ames GF. Characterization of the adenosine triphosphatase activity of the periplasmic histidine permease, a traffic ATPase (ABC transporter). *J Biol Chem* 1997;272:21883–21891. [PubMed: 9268321]
34. Bohl E, Shuman H, Boos W. Mathematical Treatment of the Kinetics of Binding Protein Dependent Transport Systems Reveals that Both the Substrate Loaded and Unloaded Binding Proteins Interact with the Membrane Components. *J Theor Biol* 1995;172:83–94. [PubMed: 7891451]
35. Merino G, Boos W, Shuman H, Bohl E. The inhibition of maltose transport by the unliganded form of the maltose-binding protein of *Escherichia coli*: experimental findings and mathematical treatment. *J Theor Biol* 1995;177:171–179. [PubMed: 8558904]
36. Jacso T, Grote M, Daus M, Schmieder P, Keller S, Schneider E, Reif B. The periplasmic loop P2 of the MalF subunit of the maltose ATP binding cassette transporter is sufficient to bind the maltose binding protein MalE. *Biochemistry*. 2009
37. Marvin JS, Hellinga HW. Manipulation of ligand binding affinity by exploitation of conformational coupling. *Nat Struct Biol* 2001;8:795–78. [PubMed: 11524684]
38. Newcomer ME, Lewis BA, Quioco FA. The radius of gyration of L- arabinose-binding protein decreases upon binding of ligand. *J Biol Chem* 1981;256:13218–13222. [PubMed: 7031058]
39. Shilton B, Flocco M, Nilsson M, Mowbray S. Conformational changes of three periplasmic receptors for bacterial chemotaxis and transport: the maltose-, glucose/galactose- and ribose-binding proteins. *J Mol Biol* 1996;264:350–363. [PubMed: 8951381]
40. Hall JA, Thorgeirsson TE, Liu J, Shin YK, Nikaido H. Two modes of ligand binding in maltose-binding protein of *Escherichia coli*. Electron paramagnetic resonance study of ligand-induced global conformational changes by site-directed spin labeling. *J Biol Chem* 1997;272:17610–17614. [PubMed: 9211909]
41. Shilton BH. The dynamics of the MBP-MalFGK(2) interaction: a prototype for binding protein dependent ABC-transporter systems. *Biochim Biophys Acta* 2008;1778:1772–1780. [PubMed: 17950243]
42. Merino G, Shuman HA. Unliganded maltose-binding protein triggers lactose transport in an *Escherichia coli* mutant with an alteration in the maltose transport system. *J Bacteriol* 1997;179:7687–7694. [PubMed: 9401026]

43. Sharff A, Rodseth L, Spurlino J, Quioco F. Crystallographic Evidence of a Large Ligand-Induced Hinge-Twist Motion between the Two Domains of the Maltodextrin Binding Protein Involved in Active Transport and Chemotaxis. *Biochemistry* 1992;31:10657–10663. [PubMed: 1420181]
44. Spurlino JC, Lu GY, Quioco FA. The 2.3-Å resolution structure of the maltose- or maltodextrin-binding protein, a primary receptor of bacterial active transport and chemotaxis. *J Biol Chem* 1991;266:5202–5219. [PubMed: 2002054]



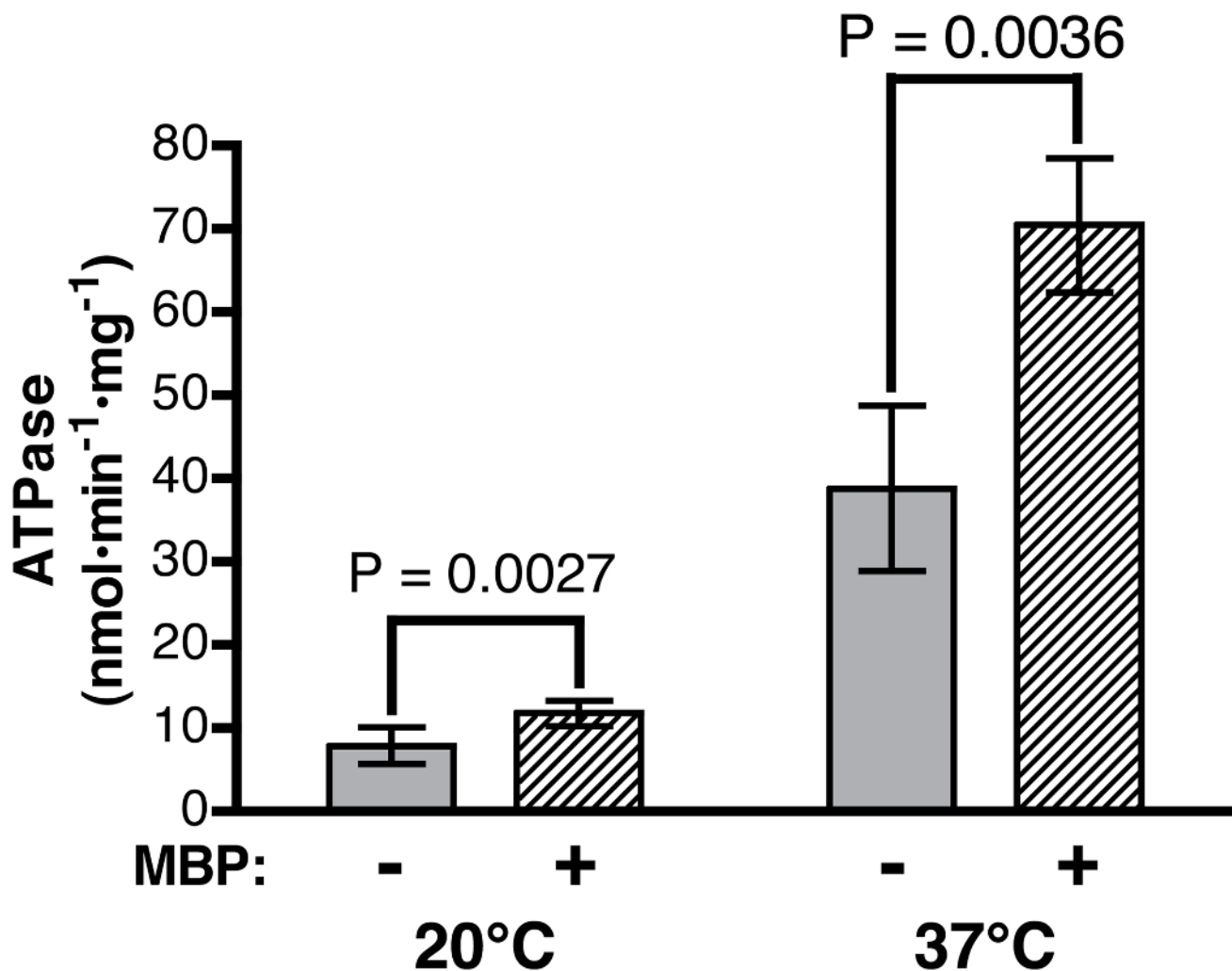


**Figure 1. Stimulation of the MalFGK<sub>2</sub> ATPase by unliganded MBP**

ATP hydrolysis was measured for proteoliposomes on their own (solid grey bars) as well as with 2  $\mu$ M MBP (stippled bars) at 20° and 37°. The addition of MBP resulted in an 50% increase in ATPase activity at 20°, and a 100% increase at 37°C. Shown are the mean  $\pm$  S.D.; a paired t-test was used to calculate the likelihood that the differences arose by chance.

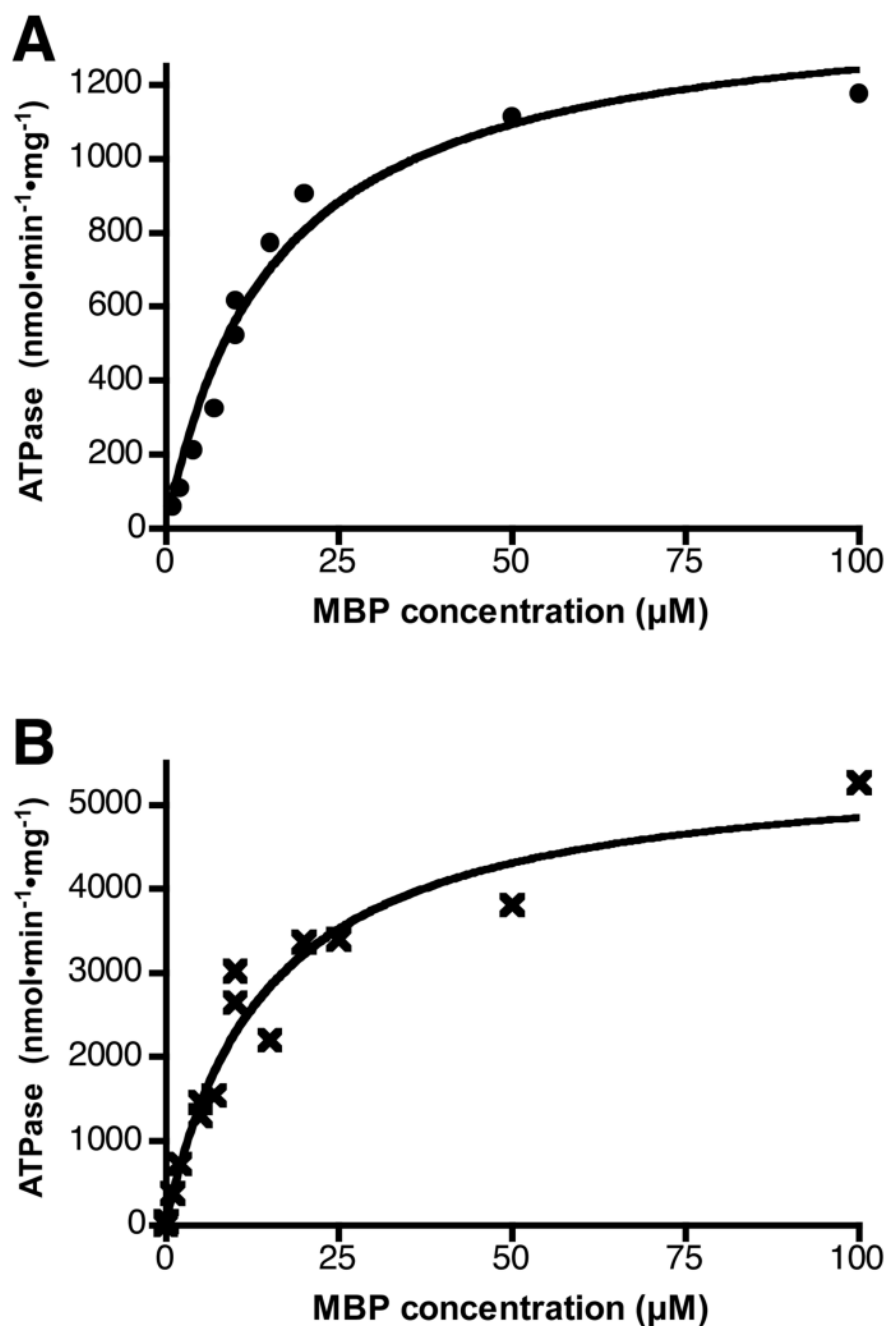


**Figure 2. Kinetic analysis of MBP-MalFGK<sub>2</sub> ATPase stimulation in the presence of maltose**  
 The ability of wild-type MBP to stimulate the MalFGK<sub>2</sub> ATPase, at MBP concentrations from 2 to 100  $\mu\text{M}$ , was measured in the presence of 5 mM maltose at (A) 20°C, filled circles, and (B) 37°C, crosses. The solid curves show the non-linear least-squares fits to the Michaelis-Menten equation, which yielded  $K_M$  values (defined as the concentration of MBP that yields half maximal ATPase) of approximately 15  $\mu\text{M}$  and  $V_{\text{MAX}}$  values of 1400 and 5500  $\text{nmol}\cdot\text{min}^{-1}\cdot\text{mg}^{-1}$  at 20° and 37°, respectively (Table 1). Note that all MBP preparations included an unfolding and refolding step, as described in Methods, to completely remove ligand.

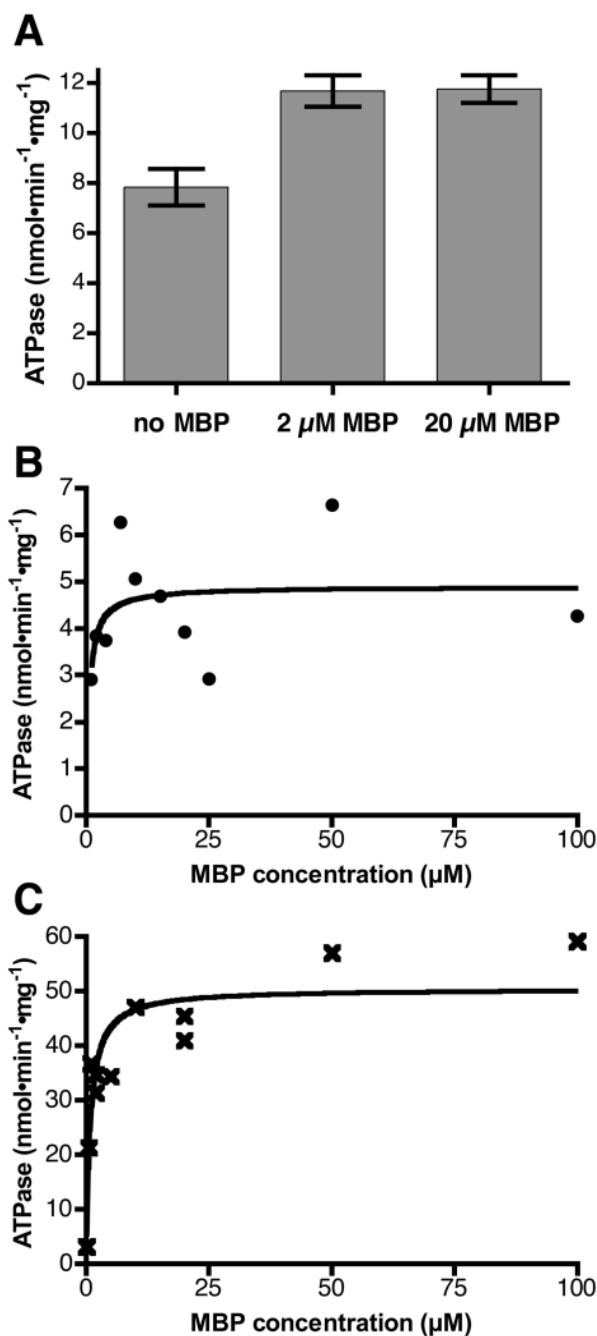


**Figure 3. Kinetic analysis of MBP-MalFGK<sub>2</sub> ATPase stimulation in the absence of maltose** (A) In the absence of maltose, MBP produces a small but significant stimulation of the MalFGK<sub>2</sub> ATPase that is exactly the same for 2 μM and 20 μM concentrations of MBP at 20° C. The bars show the mean ± S.D. for 6 to 9 determinations in each case. (B) At 20°C and in the absence of maltose, increases in MBP concentration from 1 to 100 μM produced no significant increase in MalFGK<sub>2</sub> ATPase activity (filled circles). Note that activities below 1 μM MBP concentration could not be reliably determined at 20°C. (C) At 37°C and in the absence of maltose, the higher activity levels allowed measurement of the MalFGK<sub>2</sub> ATPase activity at MBP concentrations below 1 μM (crosses). The data in panels B and C yielded  $K_M$  values of less than 1 μM and  $V_{MAX}$  values of 5 and 50 nmol·min<sup>-1</sup>·mg<sup>-1</sup> at 20° and 37°,

respectively. For the analysis in panels B and C, the basal ATPase of the proteoliposomes (in the absence of any MBP) was subtracted from all measurements.

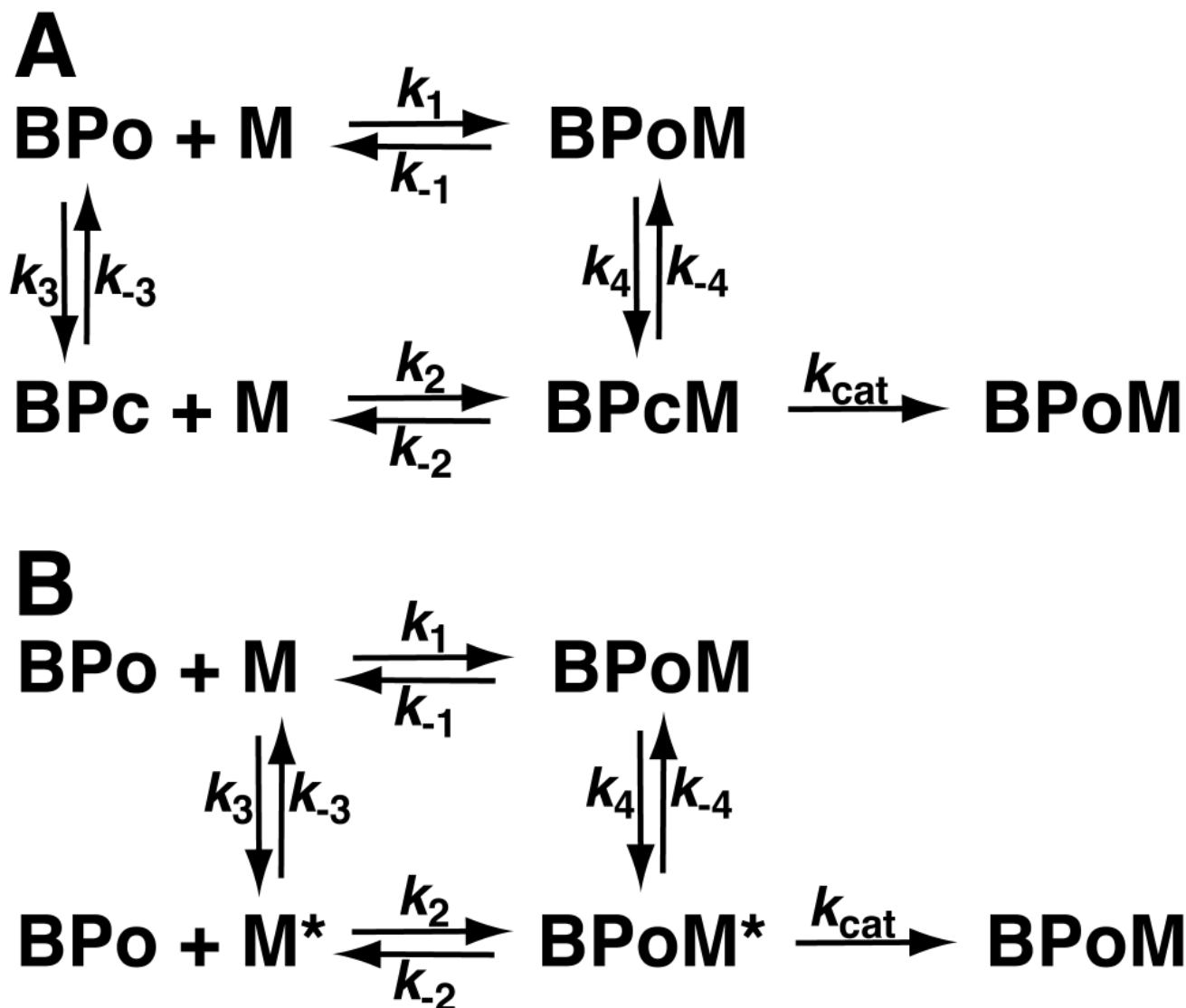


**Figure 4. Kinetic models for stimulation of MalFGK<sub>2</sub> ATPase by open and closed MBP**  
 (A) Stimulation by closed MBP. Both open and closed forms of MBP (BPo and BPc, respectively) interact with MalFGK<sub>2</sub> but only the closed form stimulates ATP hydrolysis. In this model, the mechanism of ATPase stimulation is the same for both unliganded and liganded MBP: the closed conformation interacts with MalFGK<sub>2</sub> leading to ATP hydrolysis. In the absence of maltose, the relatively low rate of ATP hydrolysis is due to the limiting concentration of closed, unliganded MBP. (B) Stimulation by open MBP. The stimulation is due to a second conformation of MalFGK<sub>2</sub> (M\*) that is separated from its more predominant “resting” or ground state (M) by an energetic barrier. Open unliganded MBP binds with high affinity to this form of MalFGK<sub>2</sub> which leads directly to formation of the transition state for ATP hydrolysis. In this system, the low rate of ATP hydrolysis in the absence of maltose is due to the slow rate of conversion between M and M\*. Relative values for the rate constants are provided in Table 2.

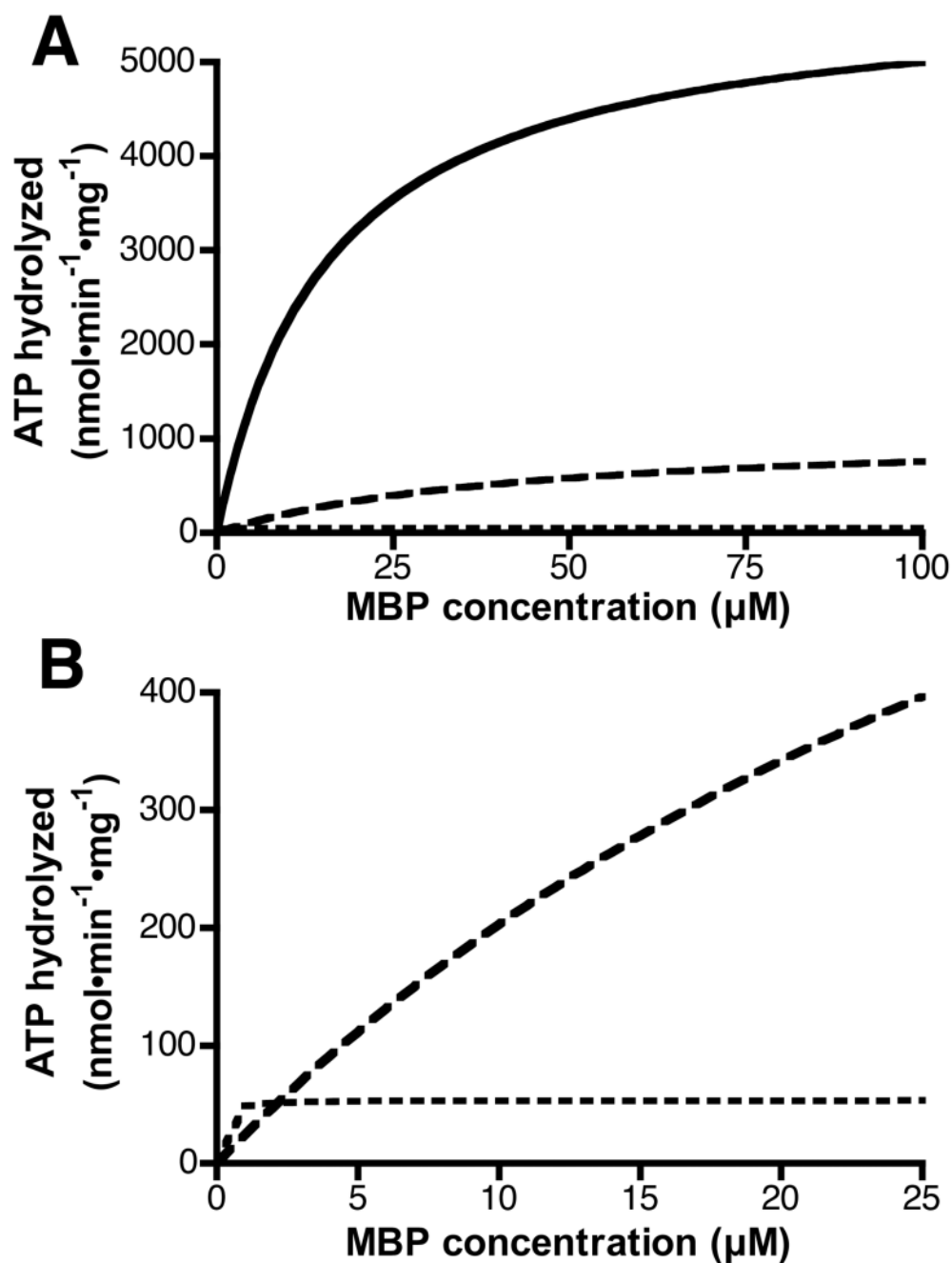


**Figure 5. Expected rate curves for MalFGK<sub>2</sub> stimulation by MBP**

The kinetic models in Figure 4 along with rate constants in Table 2 were used to derive curves for the rate of ATP hydrolysis as a function of MBP concentration. Panels A and B represent the same graphs, but with expanded axes in Panel B. In the presence of saturating maltose (solid curve), where all the binding protein is in a closed conformation (accomplished in the model by making the closed to open rate constants very small) the system shows a  $K_M$  for MBP of 15  $\mu\text{M}$ , corresponding to what was observed experimentally. In the absence of maltose, the model where the closed, unliganded form is responsible for the stimulation leads to a  $K_M$  of just over 40  $\mu\text{M}$  (long dashes) and a significant increase in activity as the concentration of MBP is raised in the region from 1 to 25  $\mu\text{M}$ . Activation by open unliganded MBP (short dashes),

as illustrated in Figure 4B and outlined in the text, yields results that are similar to what is observed experimentally.

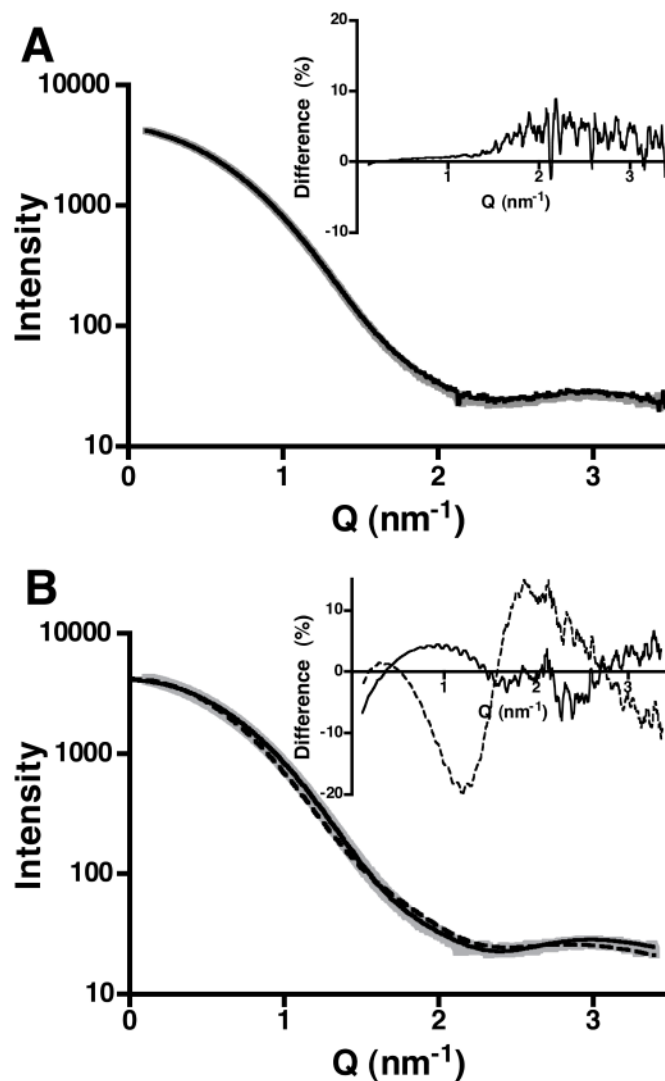


**Figure 6. Unliganded MBP-A96W/I329W is in a closed conformation**

(A) Small-angle X-ray scattering (SAXS) from MBP-A96W/I329W was measured in the absence (thick grey curve) and presence (thin black curve) of maltose. The inset graph shows the difference between the two curves, expressed as a percentage of the total signal. The two curves are almost identical, indicating no observable effect of maltose on the solution conformation of the protein. (B) The SAXS data from unliganded MBP-A96W/I329W (thick grey curve) was matched to the open structure of MBP (PDB ID 1OMP (43); dashed curve) and the closed, ligand-bound structure (PDB ID 1ANF (44); solid curve). The inset shows the difference between the models and the solution conformation of unliganded MBP-A96W/I329W as a percentage of the total signal. The closed conformation of MBP is a better model for the solution conformation of unliganded MBP-A96W/I329W.



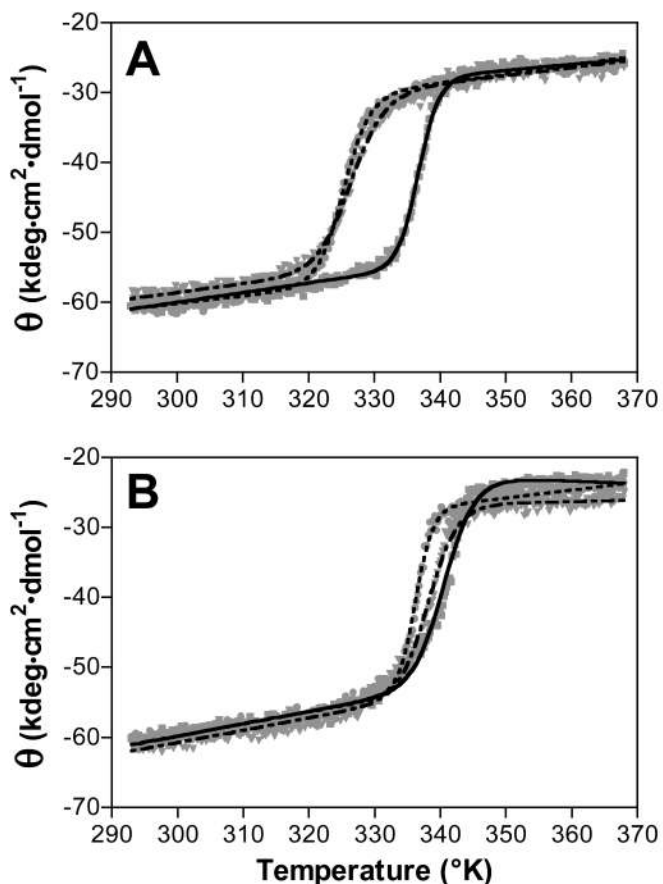


**Figure 7. Stability of conformationally engineered MBP molecules**

Conformationally engineered MBP molecules, MBP-DM and MBP-A96W/I329W, were produced by making changes in the “balancing interface” that controls opening and closing of the maltose binding cleft<sup>20,21</sup>. The thermal stabilities of MBP-DM (short dashes) and MBP-A96W/I329W (long/short dashes) were compared to wild-type MBP (solid) in the (A) absence of maltose, and (B) presence of 500  $\mu$ M maltose. The samples were heated at 75°K per hour and mean residue ellipticity ( $\theta$ ) at 222 nm was measured every 4 seconds (grey data points; squares for wild-type MBP, circles for MBP-DM, and inverted triangles for MBP-A96W/I329W). The curves are non-linear least-squares fits of the data to an equation describing thermodynamic transitions in terms of the two plateau regions (see Methods). The balancing interface mutations have decreased the stability of the unliganded conformation, but have no significant effect on the stability of the maltose-bound closed conformation.

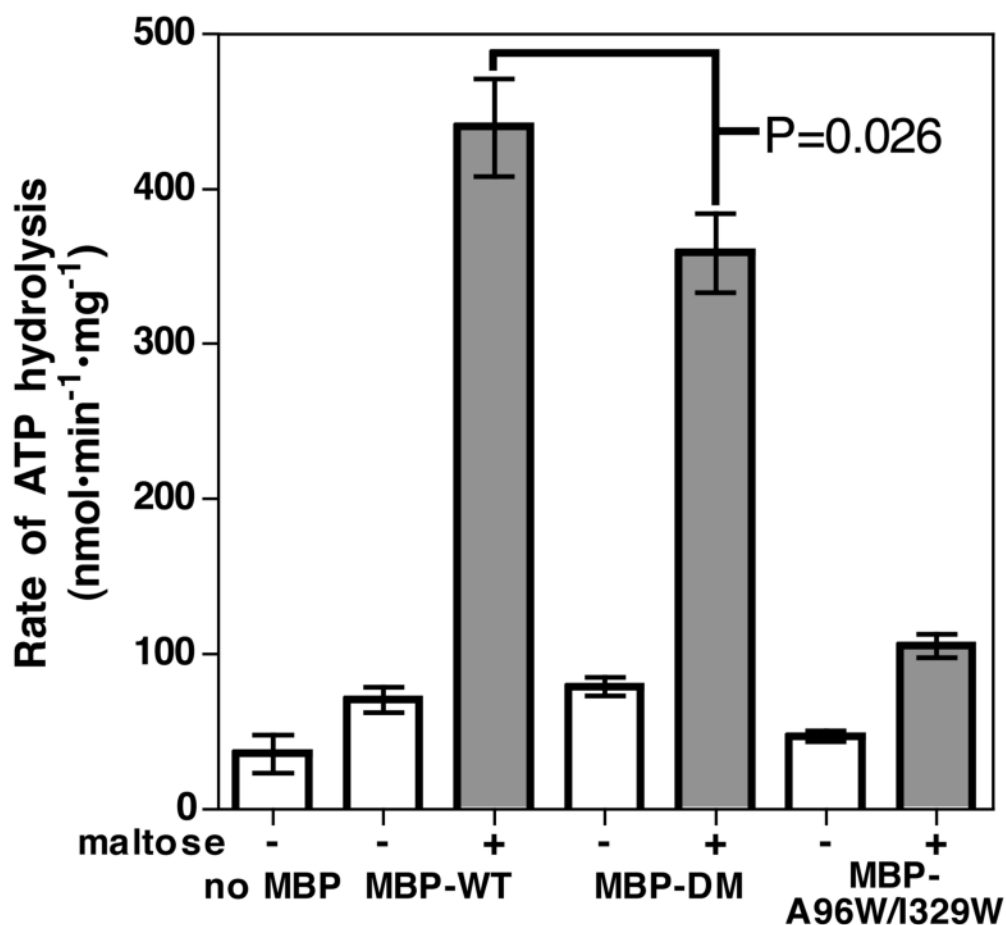


**Figure 8. Destabilization of the Open Conformation Decreases MalFGK<sub>2</sub> ATPase**

The ability of wild-type MBP (MBP-WT), MBP-DM, and MBP-A96W/I329W to stimulate the MalFGK<sub>2</sub> ATPase was measured in either the absence (hollow bars) or presence (filled bars) of 5 mM maltose. An MBP concentration of 2  $\mu$ M was used in each case, and measurements were made in triplicate; the mean value is shown with error bars representing the standard deviation. The PLS on their own (hollow bar, far left) show a low basal ATPase that is doubled by addition of unliganded MBP and increased over 10-fold by addition of MBP and maltose. In the presence of maltose, MBP-DM does not stimulate the MalFGK<sub>2</sub> ATPase to the same degree as wild-type MBP. MBP-A96W/I329W shows a severely impaired ability to stimulate MalFGK<sub>2</sub> in both the absence and presence of maltose.

**Table 1**Kinetic Parameters for Activation of MalFGK<sub>2</sub> Liganded and Unliganded MBP

Conditions <sup>a</sup>	$K_M$ ( $\mu\text{M}$ )	$V_{\text{MAX}}$ ( $\text{nmol}\cdot\text{min}^{-1}\cdot\text{mg}^{-1}$ )
Maltose-bound, 20°C	15.7 (9.4 to 22.0) <sup>b</sup>	1400 (1200 to 1700)
Unliganded, 20°C	0.57 (0 to 1.8)	4.9 (3.7 to 6.1)
Maltose-bound, 37°C	14.3 (8.1 to 20.6)	5500 (4600 to 6500)
Unliganded, 37°C	0.81 (0.17 to 1.4)	50 (43 to 58)

<sup>a</sup>The basal ATPase activity measured in the absence of MBP was subtracted from all measurements.

<sup>b</sup>Values in parentheses indicate the 95% confidence interval, as provided by the Prism software.

**Table 2**

Rate Constants for Kinetic Models

Parameter	Stimulation by Closed MBP		Stimulation by Open Unliganded MBP
	Maltose Saturated	Closed Unliganded	
$k_1$	1	1	1
$k_{-1}$	50	50	50
$k_2$	1	1	1
$k_{-2}$	15	15	0.015
$k_3$	1	1	0.01
$k_{-3}$	0.01	10	0.1
$k_4$	1	1	0.01
$k_{-4}$	0.01	10	0.1
$k_{cat}$	1	1	1